Electronic Supplementary Information

Data analytics accelerates the experimental discovery of $Cu_{1-x}Ag_xGaTe_2$ based thermoelectric chalcogenides with high figure of merit

Yaqiong Zhong,[#a,f] Xiaojuan Hu,[#b] Debalaya Sarker,[#c,d] Xianli Su,[e] Qingrui Xia,[a,f] Liangliang Xu,[g] Chao Yang,[a,f] Xinfeng Tang,[e] Sergey V. Levchenko,*[c] Zhongkang Han*[c,h] and Jiaolin Cui*[a]

[a] School of Materials and Chemical Engineering, Ningbo University of Technology, Ningbo 315211, China
[b] Fritz-Haber-Institute of the Max Planck Society, Berlin 14195, Germany
[c] Center for Energy Science and Technology, Skolkovo Institute of Science and Technology, Moscow 413026, Russia
[d] UGC-DAE Consortium for Scientific Research Indore, Khandwa Road, Indore 452001, India
[e] State Key Laboratory of Advanced Technology for Materials Synthesis and Processing, Wuhan University of Technology, Wuhan 430070, China
[f] School of Materials Science and Engineering, China University of Mining and Technology, Xuzhou 221116, China
[g] Multidisciplinary Computational Laboratory, Department of Electrical and Biomedical Engineering, Hanyang University, Seoul 04763, Korea
[h] State Key Laboratory of Silicon Materials, School of Materials Science and Engineering, Zhejiang University, Hangzhou, 310027, China
[#] These authors contributed equally.

Correspondence Email: S.Levchenko@skoltech.ru; hanzk@zju.edu.cn; cuijl@nbut.edu.cn

Supplementary methods

To construct the Φ_1 and Φ_2 feature spaces, we made use of the set of algebraic/functional operators given in eq. 1.

$$\hat{H}^{(m)} \equiv \{+, -, \cdot, /, \log, \exp, \exp-, ^{-1}, ^{2}, ^{3}, \sqrt{}, ^{3}\sqrt{}, |-|\}. \quad (1)$$

The superscript m indicates that when applying $\hat{H}^{(m)}$ to primary features φ_1 and φ_2, a dimensional analysis is performed, which ensures that only physically meaningful combinations are retained (e.g., only primary features with the same units are added or subtracted). All primary features included in this study were obtained from the literature[1]. The values of the primary features for the training datasets at each iteration can be found in the file "Supplementary Data".

The sparsifying ℓ_0 constraint is applied to a smaller feature subspace selected by a screening procedure (sure independence screening (SIS)), where the size of the subspace is equal to a user-defined SIS value times the dimension of the descriptor. The SIS value is not an ordinary hyperparameter, and its optimization through a validation dataset is not straightforward. Ideally, one would want to search the entire feature space for the optimal descriptor. However, this is not computationally tractable since the computational cost of the sparsifying ℓ_0 constraint exponentially grows with the size of the searched feature space. Instead, the SIS value should be chosen to be as large as computationally possible. Reasonable SIS values were chosen based on the convergence of the training error.

High-throughput (HT) screening of the very large compositional space of ternary-based chalcogenide materials $A_{1-x}A^*_xB_{1-y}B^*_yC_{2-z}C^*_z$ (where A = Cu or Ag; B = Bi, In, Sb, or Ga; C = Se or Te; A* = Cu, Ag, Zn, or Na; B* = Ga, In, Bi, Sb, Zn, or Sn; and C* = Te or Cl) was performed. The mixtures of $CuInTe_2$, $CuGaTe_2$, $AgInTe_2$, and $AgGaTe_2$ are stable over a large temperature range according to the literature[2-5]. Thus, their mixtures were also included in our high-throughput screening.

Table S1 Values of all primary features.

Element	HF (eV)	HV (eV)	EN	IE (eV)	AW (amu)	AR (Å)
Cu	0.14	3.11	1.90	7.73	63.55	1.28
Ag	0.12	2.63	1.93	7.58	107.87	1.44
Ga	0.06	2.65	1.81	6.00	69.72	1.35
In	0.03	2.40	1.78	5.79	114.82	1.67
Bi	0.12	1.86	2.02	7.29	208.98	1.56
Sb	0.21	2.00	2.05	8.64	121.76	1.40
Te	0.18	1.18	2.10	9.01	127.60	1.40
Se	0.07	0.99	2.55	9.75	78.97	1.20
Sn	0.07	3.07	1.96	7.34	118.71	1.40
Cl	0.07	0.21	3.16	12.97	35.45	0.99
Na	0.03	1.01	0.93	5.14	22.99	1.86
Zn	0.08	1.19	1.65	9.39	65.38	1.34

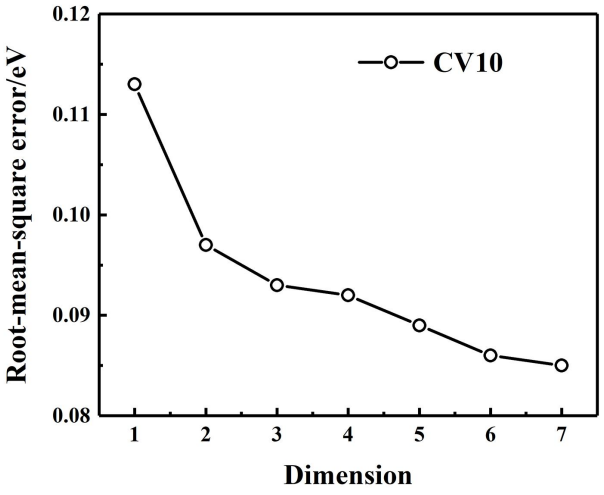

Fig. S1 CV10 error of the SISSO model.

Table S2 zT values from previous reports on chalcogenide materials from other groups along with the SISSO-predicted values.

system	temperature (K)	SISSO-predicted	previously reported
$CuGaTe_2$	950	1.48	1.40[6]
$Cu_{0.7}Ag_{0.3}In_{0.6}Ga_{0.4}Te_2$	873	1.30	1.64[2]
$AgSb_{0.98}Bi_{0.02}Se_2$	680	0.66	1.15[7]
$AgSbTe_2$	533	0.81	1.55[8]
$AgBiSe_2$	700	0.46	1.50[9]
$AgSb_{0.96}Zn_{0.04}Te_2$	585	1.16	1.90[10]
$AgSbTe_{1.98}Se_{0.02}$	565	0.83	1.37[11]
$AgSbTe_{1.85}Se_{0.15}$	575	0.84	2.10[12]
$AgSb_{0.93}In_{0.07}Te_2$	650	0.88	1.35[13]

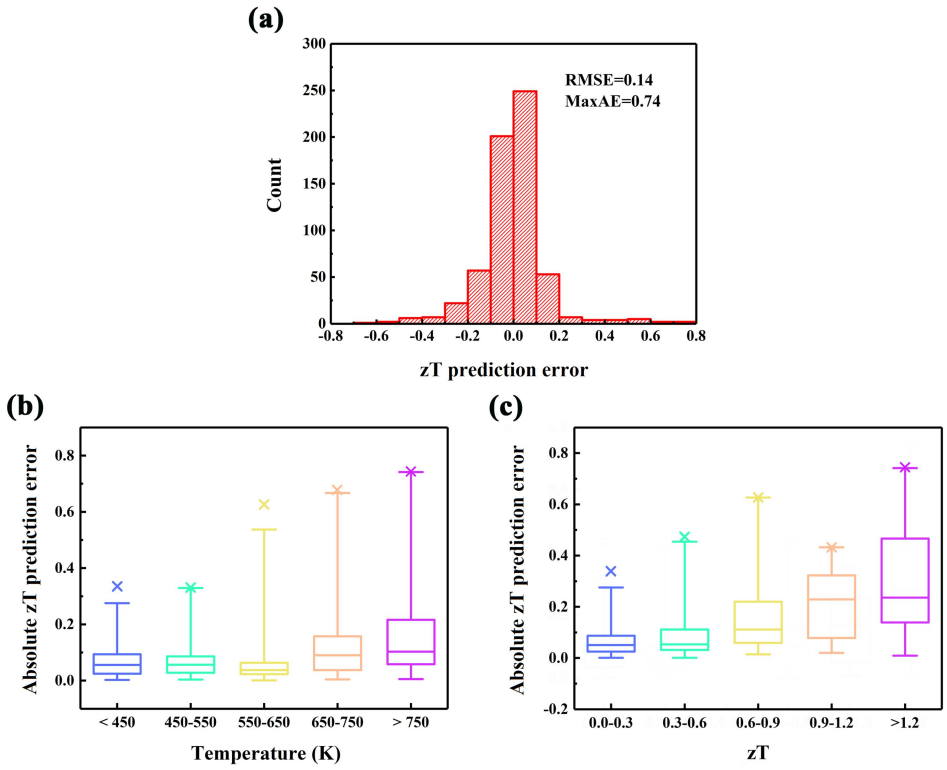

Fig. S2 (a) Distribution of zT prediction errors for the best SISSO model. (b) and (c) Box plots of the error distribution as a function of temperature range and zT range, respectively. The upper and lower limits of the rectangles show the 75th and 25th percentiles of the distributions, the internal horizontal lines mark the median (50th percentile), and the upper and lower limits of the error bars indicate the 99th and 1st percentiles of the distributions. The crosses represent the maximum errors.

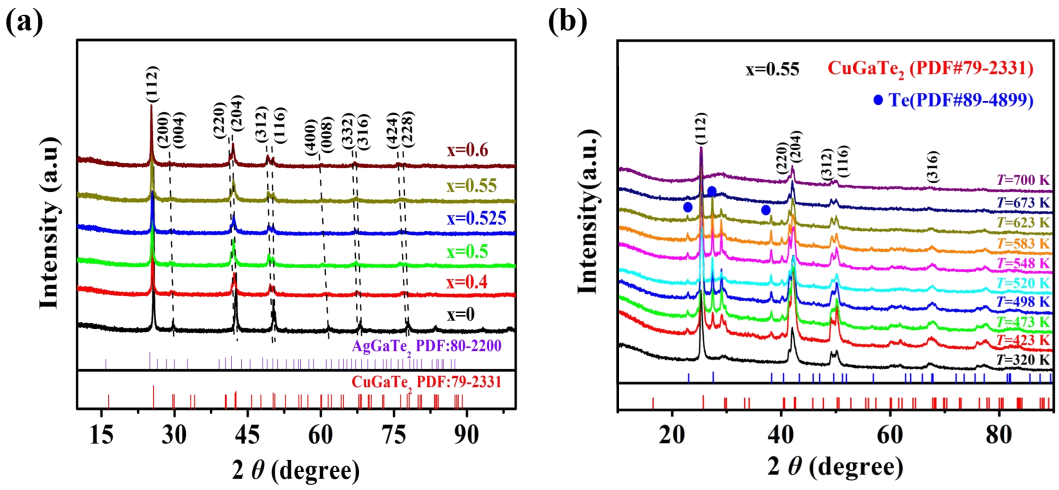

Fig. S3 (a) Powder XRD patterns for $Cu_{1-x}Ag_xGaTe_2$ (x=0.4-0.6) at room temperature, where the pattern of the sample with x=0 is provided for comparison. The XRD peaks show a shifting trend with increasing x. (b) High-temperature XRD patterns for $Cu_{0.45}Ag_{0.55}GaTe_2$.

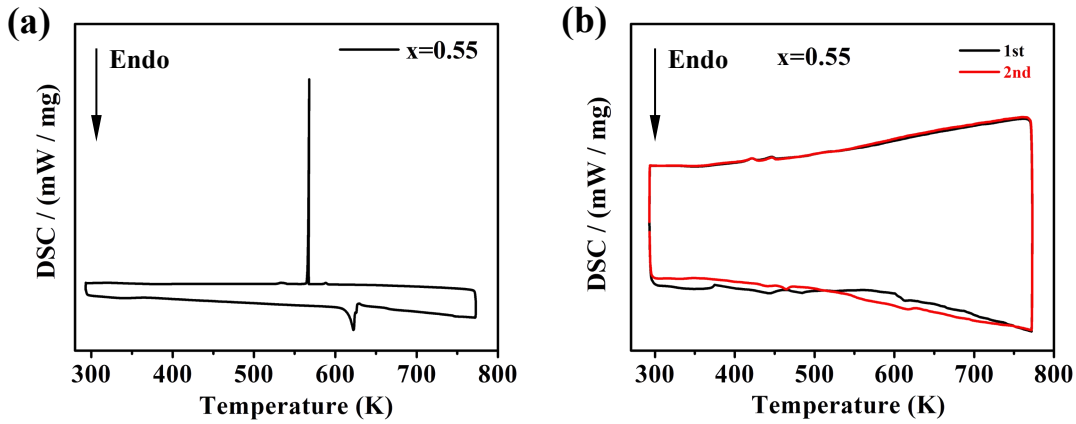

Fig. S4 DSC signal as a function of temperature for the bulk material $Cu_{0.45}Ag_{0.55}GaTe_2$: (a) Before measurement, and (b) After measurement.

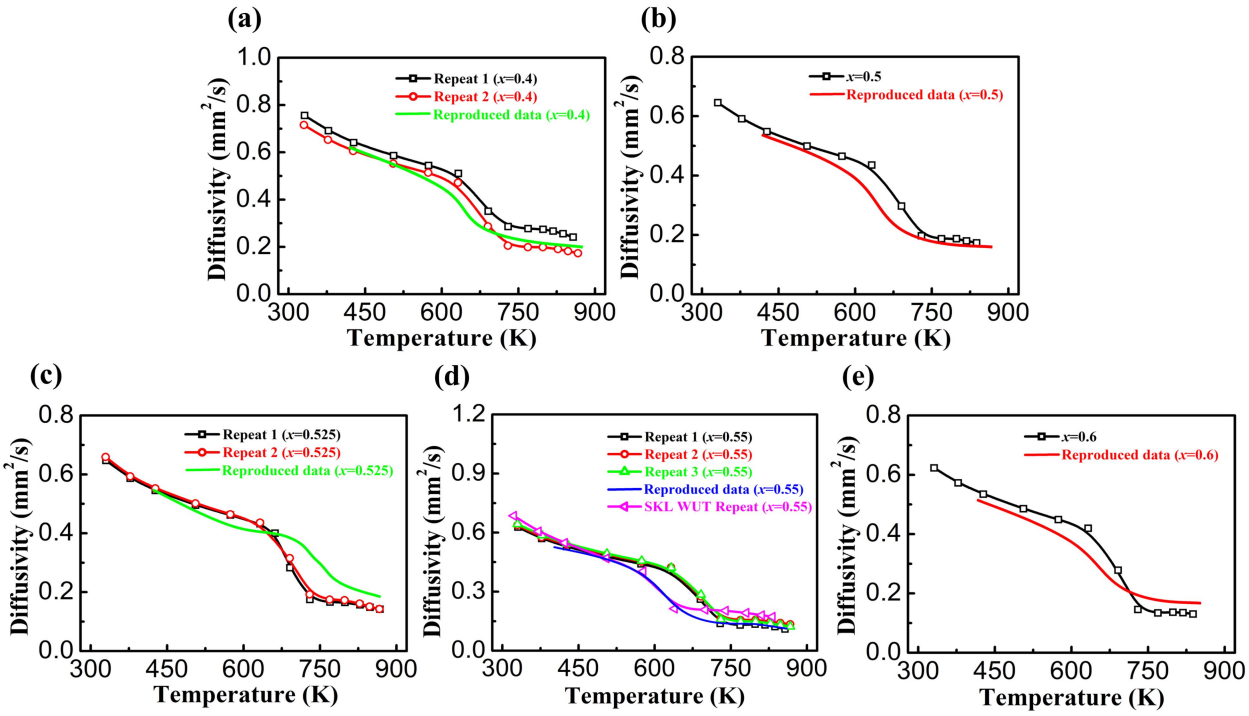

Fig. S5 Thermal diffusivity as a function of temperature for $Cu_{1-x}Ag_xGaTe_2$ (x=0.4-0.6): (a) x=0.4; (b) x=0.5; (c) x=0.525; (d) x=0.55 ($Cu_{0.45}Ag_{0.55}GaTe_2$ was checked by the State Key Laboratory of Advanced Technology for Materials Synthesis and Processing at Wuhan University of Technology (SKL WUT)); and (e) x=0.6. (the data shown as solid lines were reproduced by the Center for Materials Research and Analysis at Wuhan University of Technology (CMRA WUT), see the Supplementary Appendix).

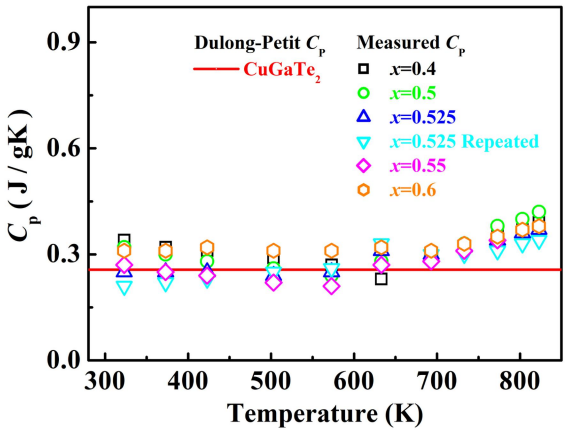

Fig. S6 Measured heat capacities (C_p) as a function of temperature for $Cu_{1-x}Ag_xGaTe_2$ (x=0.4-0.6).

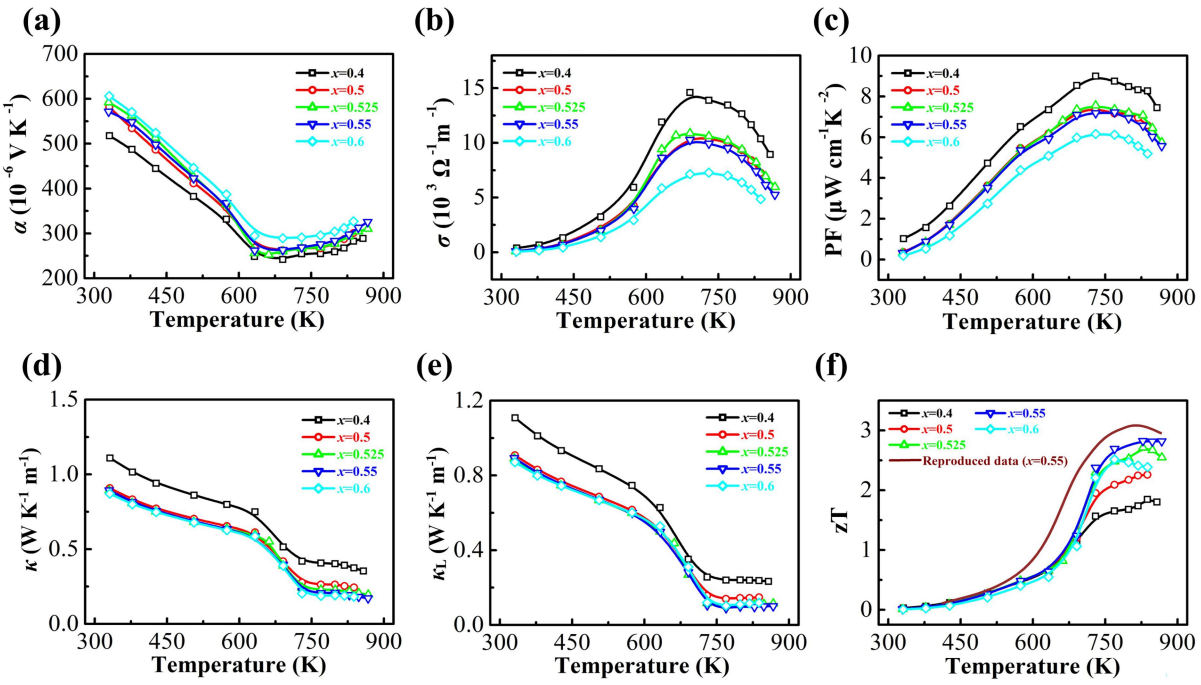

Fig. S7 Physical parameters of the bulk $Cu_{1-x}Ag_xGaTe_2$ (x=0.4-0.6) as a function of temperature: (a) Seebeck coefficients (α); (b) Electrical conductivities (σ); (c) PFs; (d) Total thermal conductivities (κ) obtained using the C_p estimated form Dulong-Petit model; (e) Lattice thermal conductivities (κ_L); and (f) Figure of merit (zT) calculated using κ shown in panel d. The wine line in panel f is the reproduced data from CMRA WUT for comparison.

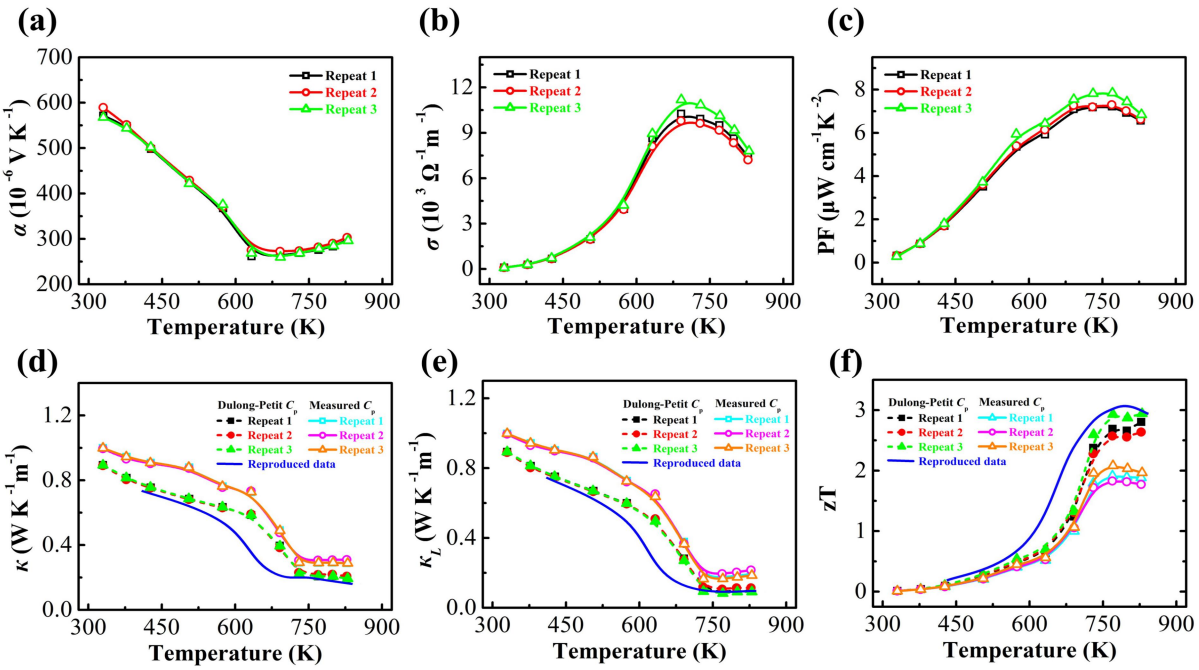

Fig. S8 Repeated measurements of TE properties as a function of temperature for $Cu_{0.45}Ag_{0.55}GaTe_2$. (a) Seebeck coefficients (α); (b) Electrical conductivities (σ); (c) PFs; (d) Total thermal conductivities (κ); (e) Lattice thermal conductivities (κ_L); and (f) Figure of merit (zT). The solid lines in Supplementary Fig. 8d-f represent the data obtained using the measured C_p, while the dotted lines represent the data obtained using the Dulong-Petit approximated C_p. The blue lines in panels d-f represent the reproduced data from CMRA WUT.

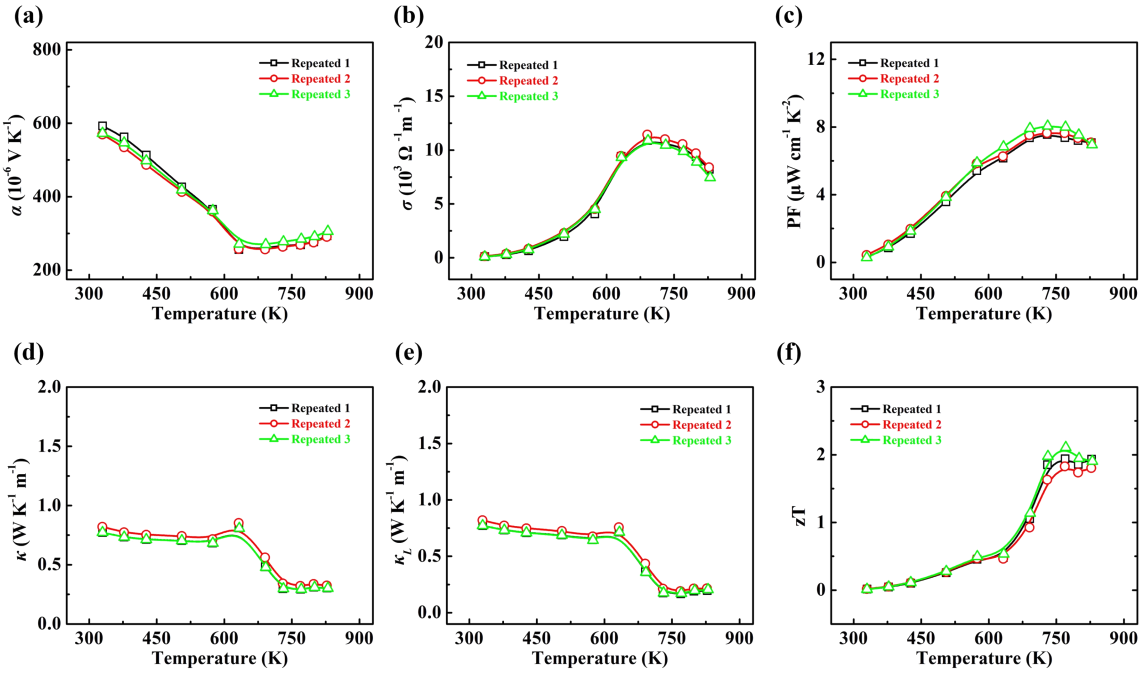

Fig. S9 Repeated measurements of TE properties as a function of temperature for $Cu_{0.475}Ag_{0.525}GaTe_2$. (a) Seebeck coefficients (α); (b) Electrical conductivities (σ); (c) PFs; (d) Total thermal conductivities (κ); (e) Lattice thermal conductivities (κ_L); and (f) Figure of merit (zT). The values were obtained using the measured C_p.

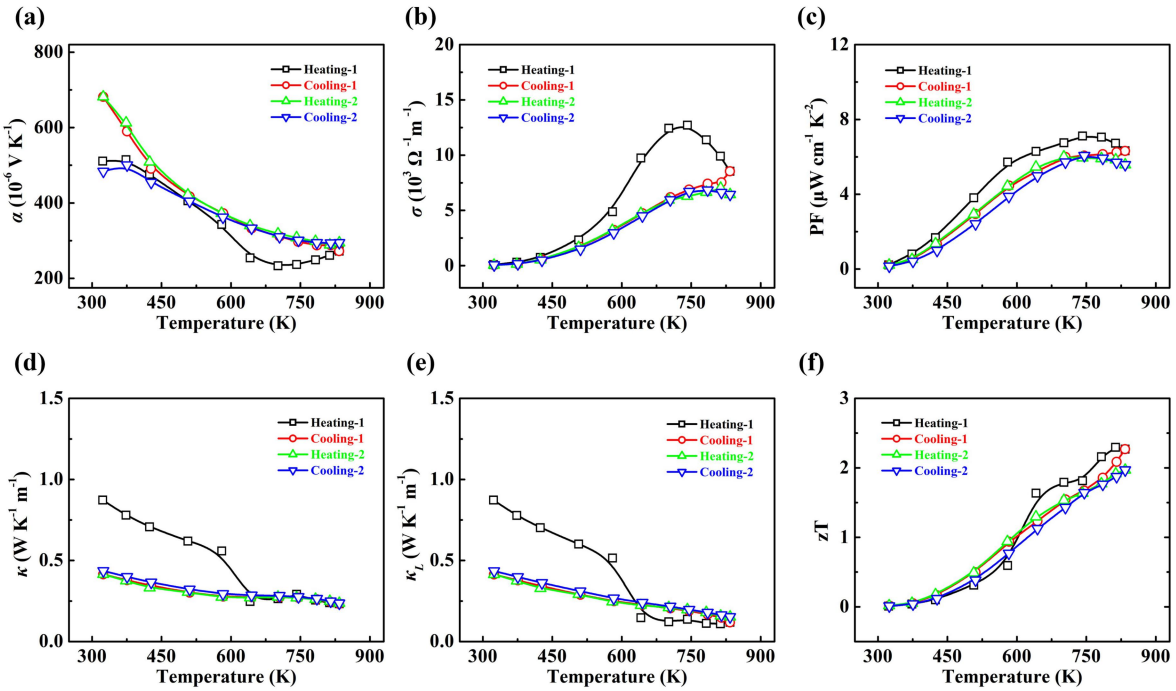

Fig. S10 TE properties as a function of temperature for $Cu_{0.475}Ag_{0.525}GaTe_2$ under two heating-cooling cycling measurements. (a) Seebeck coefficients (α); (b) Electrical conductivities (σ); (c) PFs; (d) Total thermal conductivities (κ); (e) Lattice thermal conductivities (κ_L); and (f) Figure of merit (zT). The total (κ) and lattice (κ_L) thermal conductivities were obtained using the measured C_p; see the Methods section in the main text. The cycling measurements were carried out by SKL WUT.

Supplementary appendix

Test report for the thermal diffusivity from the Center for Materials Research and Analysis at Wuhan University of Technology.

编号：20210008

武汉理工大学材料研究与测试中心

数 据 报 告

样品名称：$Cu(Ag)GaTe_2$

送样单位：宁波工程学院（Ningbo University of Technology）

通讯地址：浙江省宁波市江北区风华路 201 号

检测单位（盖章）：武汉理工大学材料研究与测试中心

发送日期 2021 年 1 月 11 日

地址：武汉市武昌珞狮路 122 号
邮政编码： 430070
网址：http://cmra.whut.edu.cn/
电话：027－87651843
传真：027－87878641
Email：junyl@whut.edu.cn

检 测 数 据

报告编号：20210008 共 1 页 第 1 页（其中图 0 页，表 1 页）

样品编号	202100081701~05			检验类别	委托送样
样品名称	Cu(Ag)$GaTe_2$				
样品状态	黑色固体	接样时间	2021/1/5	检测时间	2021/1/6~1/7
检测项目	热扩散系数				
参考依据	GB/T 22588－2008 闪光法测量热扩散系数或导热系数				
检测设备	激光导热仪(LFA457)			设备编号	1604780S
检测条件	室温:22℃，湿度:32%RH；检测温度范围：室温～580℃，激光电压：1538V，气氛：Ar，流量：80mL/min。				

检测结果

检测项目 / 样品编号（名称）	热扩散系数（mm^2/s）						
	室温	150℃	300℃	400℃	500℃	550℃	580℃
202100081701 $(CuGaTe_2)_{0.6}(AgGaTe_2)_{0.4}$	0.80	0.61	0.49	0.26	0.23	0.22	0.20
202100081702 $(CuGaTe_2)_{0.5}(AgGaTe_2)_{0.5}$	0.68	0.53	0.42	0.21	0.18	0.17	0.16
202100081703 $(CuGaTe_2)_{0.475}(AgGaTe_2)_{0.525}$	0.72	0.55	0.43	0.41	0.28	0.22	0.20
202100081704 $(CuGaTe_2)_{0.45}(AgGaTe_2)_{0.55}$	0.65	0.50	0.35	0.16	0.14	0.12	0.12
202100081705 $(CuGaTe_2)_{0.4}(AgGaTe_2)_{0.6}$	0.66	0.50	0.39	0.22	0.19	0.17	0.16

以下空白

检测人：卓慧卿 校核人：杨新a 报告批准人：郝水援

签发日期 2021 年 1 月 11 日

No. 20210008

Center for Materials Research and Analysis in Wuhan University of Technology.

TEST REPORT

Sample Name: $Cu(Ag)GaTe_2$

Client: Ningbo University of Technology

Address: No. 201, Fenghua Road, Jiangbei District, Ningbo, Zhejiang.

Inspection Agency: Center for Materials Research and Analysis in Wuhan University of Technology

Address: 122 Luoshi Road,Wuhan,Hubei, P.R.China **Telephone:** 027-87651843

Postcode: 430070 **Fax:** 027-87878641

Website address: http://cmra.whut.edu.cn/ **Email:** junyl@whut.edu.cn

TEST DATA

No. 20210008 **Page 1 of 1**

Sample No.	202100081701~05			**Test Type**	Sample delivery
Name	$Cu(Ag)GaTe_2$				
Sample Status	Black solid	**Receiving Date**	January 5, 2021	**Testing Date**	January 6~7, 2021
Test Item	Thermal diffusivity				
Reference Standards	GB/T 22588-2008 Laser Flash Method to measure thermal diffusivity or thermal conductivity				
Instrument	LFA457			**Instrument No.**	1604780S
Test Conditions	Room temperature (RT): 22 ℃, Humidity: 32% RH, Temperature range: RT~580 ℃, Laser voltage: 1538 V, Atmosphere: Ar, Gas flow: 80 mL/min。				
Test Results					

Test Item / Sample No.	Thermal Diffusivity (mm^2/s)						
	RT	150℃	300℃	400℃	500℃	550℃	580℃
202100081701 $(CuGaTe_2)_{0.6}(AgGaTe_2)_{0.4}$	0.80	0.61	0.49	0.26	0.23	0.22	0.20
202100081702 $(CuGaTe_2)_{0.5}(AgGaTe_2)_{0.5}$	0.68	0.53	0.42	0.21	0.18	0.17	0.16
202100081703 $(CuGaTe_2)_{0.475}(AgGaTe_2)_{0.525}$	0.72	0.55	0.43	0.41	0.28	0.22	0.20
202100081704 $(CuGaTe_2)_{0.45}(AgGaTe_2)_{0.55}$	0.65	0.50	0.35	0.16	0.14	0.12	0.12
202100081705 $(CuGaTe_2)_{0.4}(AgGaTe_2)_{0.6}$	0.66	0.50	0.39	0.22	0.19	0.17	0.16

Opeator: RongHui Zhuo **Verifier**: XinYa Yang **Approver:** YanYuan Qi

January 11, 2021

Statement: The experimental data and results only provide reference data for the incoming samples, and are not used as a certification or notarization by a third-party testing agency. The center does not assume any related legal responsibilities resulting from this.

References

1. J. G. Speight, *Lange's Handbook of Chemistry* (McGraw-Hill Education, 2017).
2. J. Zhang, L. L. Huang, C. Zhu, C. J. Zhou, B. Jabar, J. M. Li, X. G. Zhu, L. Wang, C. J. Song, H. X. Xin, D. Li and X. Y. Qin, *Adv. Mater.,* 2019, **31**, 1905210.
3. H. Y. Xie, E. S. Bozin, Z. Li, M. Abeykoon, S. Banerjee, J. P. Male, G. J. Snyder, C. Wolverton, S. J. L. Billinge and M. G. Kanatzidis, *Adv. Mater.,* 2022, **34**, 2202255.
4. H. Y. Xie, Y. K. Liu, Y. Y. Zhang, S. Q. Hao, Z. Li, M. Cheng, S. T. Cai, G. J. Snyder, C. Wolverton, C. Uher, V. P. Dravid and M. G. Kanatzidis, *J. Am. Chem. Soc.,* 2022, **144**, 9113–9125.
5. H. Y. Xie, Z. Li, Y. K. Liu, Y. Y. Zhang, C. Uher, V. P. Dravid, C. Wolverton and M. G. Kanatzidis, *J. Am. Chem. Soc.,* 2023, **145**, 3211–3220.
6. T. Plirdpring, K. Kurosaki, A. Kosuga, T. Day, S. Firdosy, V. Ravi and G. J. Snyder, *Adv. Mater.* 2012, **24**, 3622–3626.
7. S. N. Guin, A. Chatterjee, D. S. Negi, R. Datta and K. Biswas, *Energy Environ. Sci.,* 2013, **6**, 2603–2608.
8. J. J. Xu, H. Li, B. L. Du, X. F. Tang, Q. J. Zhang and C. Uher, *J. Mater. Chem.,* 2010, **20**, 6138–6143.
9. C. Xiao, X. M. Qin, J. Zhang, R. An, J. Xu, K. Li, B. X. Cao, J. L. Yang, B. J. Ye and Y. Xie, *J. Am. Chem. Soc.,* 2012, **134**, 18460–18466.
10. S. Roychowdhury, R. Panigrahi, S. Perumal and K. Biswas, *ACS Energy Lett.,* 2017, **2**, 349–356.
11. B. L. Du, H. Li, J. J. Xu, X. F. Tang and C. Uher, *Chem. Mater.,* 2010, **22**, 5521–5527.

12. M. Hong, Z. G. Chen, L. Yang, Z. M. Liao, Y. C. Zou, Y. H. Chen, S. Matsumura and J. Zou, *Adv. Energy Mater.,* 2018, **8**, 1702333.

13. R. Mohanraman, R. Sankar, K. M. Boopathi, F. C. Chou, C. W. Chu, C. H. Lee and Y. Y. Chen, *J. Mater. Chem. A,* 2014, **2**, 2839–2844.